AMERICAN SOCIETY FOR MICROBIOLOGY | Applied and Environmental Microbiology®

ENVIRONMENTAL MICROBIOLOGY

Diguanylate Cyclase and Phosphodiesterase Interact To Maintain the Specificity of Cyclic di-GMP Signaling in the Regulation of Antibiotic Synthesis in *Lysobacter enzymogenes*

Gaoge Xu,[a] Lichuan Zhou,[b] Guoliang Qian,[c] Fengquan Liu[a,d]

[a]Institute of Plant Protection, Jiangsu Academy of Agricultural Sciences, Jiangsu Key Laboratory for Food Quality and Safety-State Key Laboratory Cultivation Base, Ministry of Science and Technology, Nanjing, China

[b]Information Center, Jiangsu Academy of Agricultural Sciences, Nanjing, China

[c]College of Plant Protection, Nanjing Agricultural University, Nanjing, China

[d]College of Plant Protection/Key Laboratory of Green Prevention and Control of Tropical Plant Diseases and Pests, Ministry of Education, Hainan University, Haikou, China

ABSTRACT Cyclic dimeric GMP (c-di-GMP) is a universal second messenger in bacteria. A large number of c-di-GMP-related diguanylate cyclases (DGCs), phosphodiesterases (PDEs), and effectors are responsible for the complexity and dynamics of c-di-GMP signaling. Some of these components employ various methods to avoid undesired cross talk to maintain signaling specificity. The synthesis of the antibiotic HSAF (heat-stable antifungal factor) in *Lysobacter enzymogenes* is regulated by a specific c-di-GMP signaling pathway that includes a PDE, LchP, and a c-di-GMP effector, Clp (also a transcriptional regulator). In the present study, from among 19 DGCs, we identified a diguanylate cyclase, LchD, that participates in this pathway. Subsequent investigation indicates that LchD and LchP physically interact and that the catalytic center of LchD is required for both the formation of the LchD-LchP complex and HSAF production. All the detected phenotypes support that LchD and LchP display local c-di-GMP signaling to regulate HSAF biosynthesis. Although direct evidence is lacking, our investigation, which shows that the interaction between a DGC and a PDE maintains the specificity of c-di-GMP signaling, suggests the possibility of the existence of local c-di-GMP pools in bacteria.

IMPORTANCE Cyclic dimeric GMP (c-di-GMP) is a universal second messenger in bacteria. The signaling of c-di-GMP is complex and dynamic, and it is mediated by a large number of components, including c-di-GMP synthases (diguanylate cyclases [DGCs]), c-di-GMP-degrading enzymes (phosphodiesterases [PDEs]), and c-di-GMP effectors. These components deploy various methods to avoid undesired cross talk to maintain signaling specificity. In the present study, we identified a DGC that interacted with a PDE to specifically regulate antibiotic biosynthesis in *L. enzymogenes*. We provide direct evidence to show that the DGC and PDE form a complex and also indirect evidence to argue that they may balance a local c-di-GMP pool to control antibiotic production. These results represent an important finding regarding the mechanism of a DGC and PDE pair to control the expression of specific c-di-GMP signaling pathways.

KEYWORDS c-di-GMP, signaling specificity, local c-di-GMP signaling, HSAF, diguanylate cyclase

Cyclic dimeric GMP (c-di-GMP), first discovered by Ross and colleagues in the mid-1980s (1), was recently shown to participate in biofilm formation, pathogenicity, the cell cycle, secondary metabolite biosynthesis, and other processes and is recognized as a ubiquitous nucleotide second messenger in bacteria (1–5). The synthesis and hydrolysis of c-di-GMP are carried out by diguanylate cyclases (DGCs) and c-di-GMP-specific phosphodiesterases (PDEs), respectively (3). DGCs, which possess a GGDEF domain, catalyze the condensation of two GTP

Editor Gladys Alexandre, University of Tennessee at Knoxville

Address correspondence to Fengquan Liu, fqliu20011@sina.com.

Received 23 September 2021
Accepted 3 November 2021
Accepted manuscript posted online 10 November 2021
Published 25 January 2022

molecules into a c-di-GMP molecule (6, 7). PDEs, which possess either an EAL or an HD-GYP domain, hydrolyze c-di-GMP into a 5′-pGpG molecule or two GMP molecules (8–11). Generally, the concentration of c-di-GMP is determined by DGCs and PDEs, and downstream effectors receive the c-di-GMP signal and generate a response. The c-di-GMP signaling pathway was considered simple until genomic analyses showed that numbers of DGCs and PDEs vary from a few to dozens in various bacteria (12). Additionally, the similarity between c-di-GMP effectors that have been identified so far, such as PilZ, GIL, and MshEN domains or inhibitory sites (I-sites) of the GGDEF domain (13–16), is limited, indicating that the c-di-GMP signaling network is large and complex.

Despite the number of c-di-GMP-related components at work, many researchers have found that several DGCs and PDEs seem to specifically participate in one or two c-di-GMP-dependent processes (17, 18). Meanwhile, more and more studies have demonstrated that physical interactions can occur among DGCs, PDEs, and particular c-di-GMP effectors (19–21). Paul and colleagues proposed that the local action of a DGC, PleD, might constitute a general regulatory principle in bacterial growth when they were studying the pole development and cell cycle of *Caulobacter crescentus* (7), and the proposal was then discussed in a review by Römling et al. (22), thus leading to the development of the concept of local c-di-GMP signaling or c-di-GMP signaling specificity.

Lysobacter enzymogenes is a soilborne, nonpathogenic, Gram-negative bacterium that can secrete the secondary metabolite HSAF (heat-stable antifungal factor), which has potent broad-spectrum antifungal activity targeting the sphingolipid biosynthesis pathway of filamentous pathogens (23–25). Therefore, we focused on the regulatory mechanism of the HSAF biosynthesis pathway, aiming to enhance the production of HSAF for use in fungal disease control as an antifungal antibiotic.

Our previous study showed that high levels of c-di-GMP inhibit HSAF production (26). A further study investigated the role of a specific c-di-GMP-dependent regulatory pathway in HSAF biosynthesis (27). In this signaling pathway, LchP, acting as a c-di-GMP PDE, and the transcriptional regulator Clp, acting as a c-di-GMP effector, physically interact (27). When LchP is activated via as-yet-unknown factors, it actively degrades c-di-GMP from the Clp–c-di-GMP complex, which leads to the release of Clp and the activation of the HSAF biosynthesis operon (27). The Clp-LchP interaction increases the PDE activity of LchP, providing positive feedback. However, our previous study described an unusual phenotype: *lchP* gene deletion resulted in only a modest increase in the intracellular c-di-GMP concentration but had a large effect on HSAF production (27). We thus aimed to investigate other factors in addition to the LchP-Clp interaction that may contribute to the maintenance of signal specificity.

In the present work, we used indirect experiments to demonstrate that LchP does not affect the global c-di-GMP concentration. Next, we identified a partner of LchP, the DGC LchD (*Lysobacter* c-di-GMP and HSAF-related diguanylate cyclase), from among 19 DGCs in *L. enzymogenes* OH11 using genetic methods. We further demonstrated that LchP and LchD physically interact and that the catalytic center of LchD is important for the LchP-LchD interaction and HSAF production. The present findings not only complement previous studies on the role of the specific c-di-GMP signaling pathway in regulating the secondary metabolite HSAF but also suggest the possibility of the existence of local c-di-GMP pools in bacteria.

RESULTS

LchP does not regulate the global c-di-GMP pool. Our previous study reported LchP as a weak PDE that regulates HSAF biosynthesis (27). To fully characterize the function of LchP, we used transcriptome sequencing (RNA-seq) to identify differentially expressed genes in the *lchP* mutant strain. Only 16 genes were differentially expressed ($\log_2$ ratio of greater than 2 or less than −2) in the *lchP* mutant strain compared to the wild-type strain, including 1 upregulated gene and 15 downregulated genes (Fig. 1A; see also Table S1 in the supplemental material). Nine of these genes belong to the HSAF biosynthesis gene cluster, and 4 have unknown functions (Fig. 1A and B). To confirm the RNA-seq data, we used quantitative real-time PCR (qRT-PCR) to determine the transcription level of the key HSAF biosynthesis gene *lafB* (Fig. 1C). The qRT-PCR results were consistent with the RNA-seq

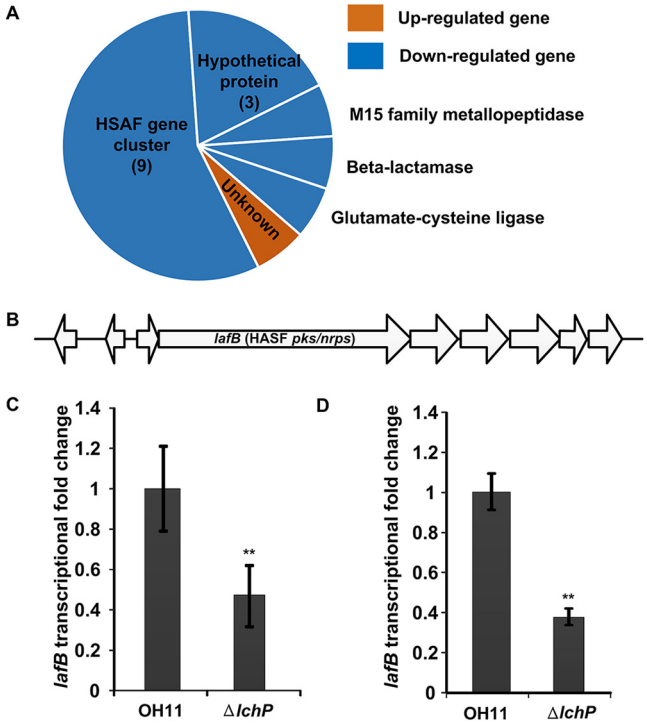

FIG 1 RNA-seq data indicate that LchP does not regulate the global c-di-GMP concentration. (A) Sixteen genes were differentially expressed in the *lchP* deletion mutant. Among these genes were 1 upregulated gene and 15 downregulated genes. (B) *lafB*, a key gene in the HSAF biosynthesis gene cluster, was downregulated in the *lchP* mutant. (C) qRT-PCR analyses of *lafB* mRNA levels in the wild-type and *lchP* mutant Δ*lchP* strains. The qRT-PCR data were obtained from three biological experiments with three technical replicates. The *lafB* mRNA level in the wild-type OH11 strain was assumed to be 1. Statistical comparisons were performed with GraphPad software (GraphPad, La Jolla, CA) using one-way ANOVA. The error bars indicate standard errors. **, $P < 0.01$ relative to wild-type OH11. (D) Transcription levels (RNA-seq data) of *lafB* in the Δ*lchP* and wild-type strains. The *lafB* mRNA level in the wild-type OH11 strain was assumed to be 1. Statistical comparisons were performed with GraphPad software (GraphPad, La Jolla, CA) using one-way ANOVA. The error bars indicate standard errors. **, $P < 0.01$ relative to wild-type OH11.

data (Fig. 1D). These results support the previous finding that LchP specifically regulates HSAF biosynthesis (27). But previous RNA-seq data showed that 775 genes, belonging to 19 functional categories, were differentially expressed (showing a ≥2-fold change) between LchP's downstream c-di-GMP effector Clp mutant strain and the wild-type strain (28), which indicates that LchP may not control the global c-di-GMP pool. Because LchP is an inner membrane-anchored protein and functions as a PDE, we hypothesized that a DGC may participate in the specific c-di-GMP signaling pathway to precisely balance the c-di-GMP concentration.

Identification of the partner DGC of LchP involved in regulating HSAF synthesis. The numbers of DGCs in bacteria vary from several to dozens (12, 29). Studies have shown that some DGCs participate in only one or two processes and coordinate their functions without excessive cross talk (17, 18). *L. enzymogenes* OH11 has 14 single GGDEF domain-containing proteins and 6 GGDEF-EAL hybrid proteins (30). Here, we hypothesized that the deficiency in HSAF production in the *lchP* mutant is caused by an increase in the c-di-GMP concentration. Thus, we aimed to determine whether the c-di-GMP level would not be increased by halting c-di-GMP synthesis and whether this manipulation would restore HSAF production. We used a genetic approach to identify the DGC that cooperates with LchP in the regulation of HSAF production. We first deleted 19 DGC-encoding genes on the background of the *lchP* mutant to generate 19 double mutants and then measured HSAF production in these mutants. The results in Fig. 2A show that only the *3756* and *lchP* double mutant produced HSAF at a level identical to that in the wild-type strain, while knockouts of the other 18 genes did not restore HSAF production or had only a small amount of recovery. Notably, both 3756 and 1158 contain the 7TMR-DISM_7TM and GGDEF domains (Fig. 2B),

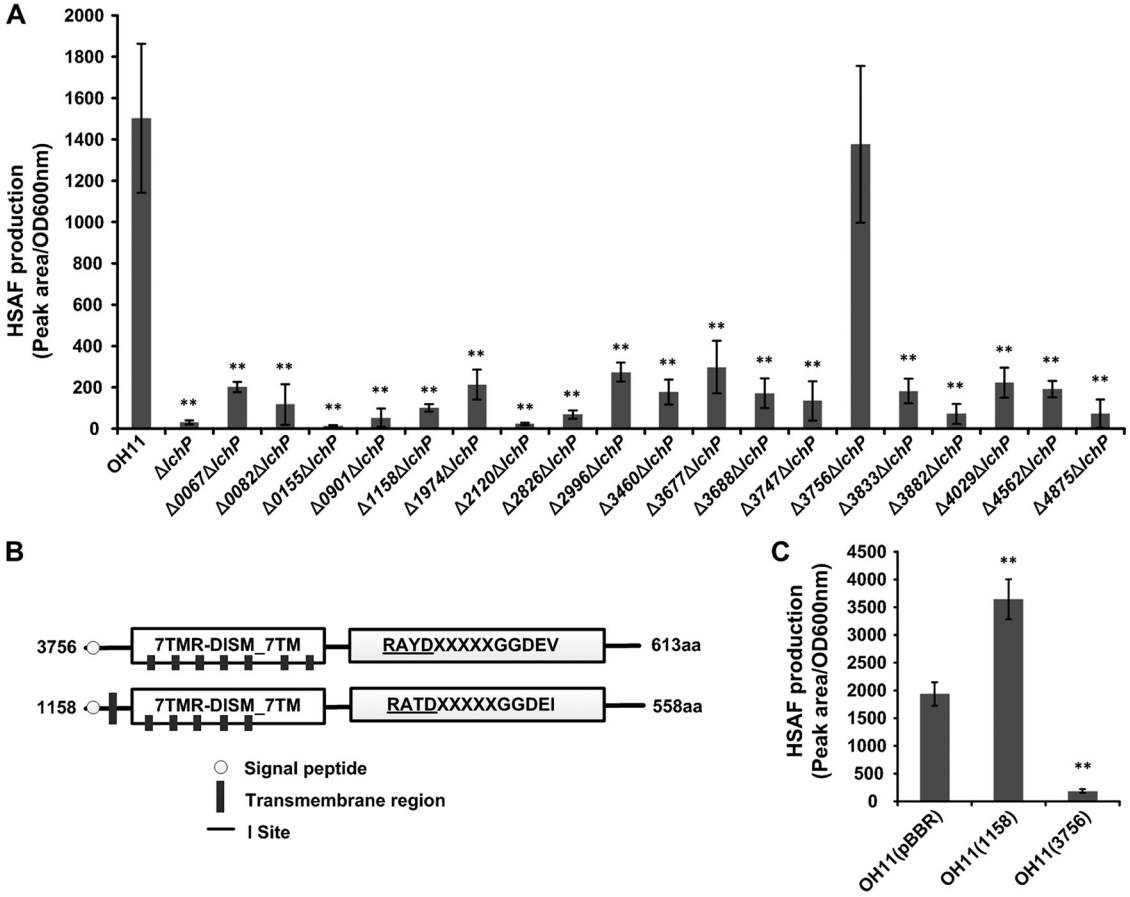

FIG 2 Identification of the partner DGC of LchP. (A) Quantification of HSAF production in the double mutants of 19 DGCs based on the *lchP* mutant. Statistical comparisons were performed with GraphPad software (GraphPad, La Jolla, CA) using one-way ANOVA. **, $P < 0.01$ relative to the wild-type OH11 strain. Biological experiments for each treatment were performed three times and assayed in triplicate. (B) Proteins 3756 and 1158 share the same domain organization. (C) Quantification of HSAF production by the overexpression of 3756 and 1158. The error bars indicate standard errors. Statistical comparisons were performed with GraphPad software (GraphPad, La Jolla, CA) using one-way ANOVA. **, $P < 0.01$ relative to the wild-type OH11 strain containing the original pBBR-MCS5 vector. Biological experiments for each treatment were performed three times and assayed in triplicate.

and multiple-sequence alignment demonstrated that they share 55% amino acid sequence similarity (Fig. S1); however, mutation of 1158 did not restore HSAF production. Additionally, the 7TMR-DISM_7TM domain is a multi-intracellular signal receptor with 7 transmembrane regions (31), indicating that 3756 is also a membrane-anchored protein with a specific location. These data suggested that 3756 is probably the DGC that partners with LchP to regulate HSAF. In another experiment, when we overexpressed 3756 in the wild-type background, HSAF production was significantly reduced (Fig. 2C), confirming our hypothesis in which an elevated c-di-GMP concentration inhibits HSAF production. However, the overexpression of 1158 increased HSAF production, indicating that 1158 may employ other mechanisms to regulate HSAF production (Fig. 2C). We renamed 3756 LchD (*Lysobacter* c-di-GMP- and HSAF-related DGC).

LchD physically interacts with LchP. We next aimed to determine why LchD, but not the similar protein 1158, is the partner of LchP. Furthermore, we wondered whether there is a connection between LchP and LchD. Do these enzymes interact? To assess these questions, we used a bacterial two-hybrid (B2H) system. In this system, the interaction of two target proteins activates the transcription of the *HIS3* reporter gene, which allows growth in the presence of 3-amino-1,2,4-triazole (3-AT), a competitive inhibitor of the His_3 enzyme. Positive results are verified by using the *aadA* gene, which confers streptomycin (Str) resistance, as a secondary reporter (32). The results in Fig. 3A show that the cytoplasmic regions of LchP and LchD interact. This interaction was further confirmed

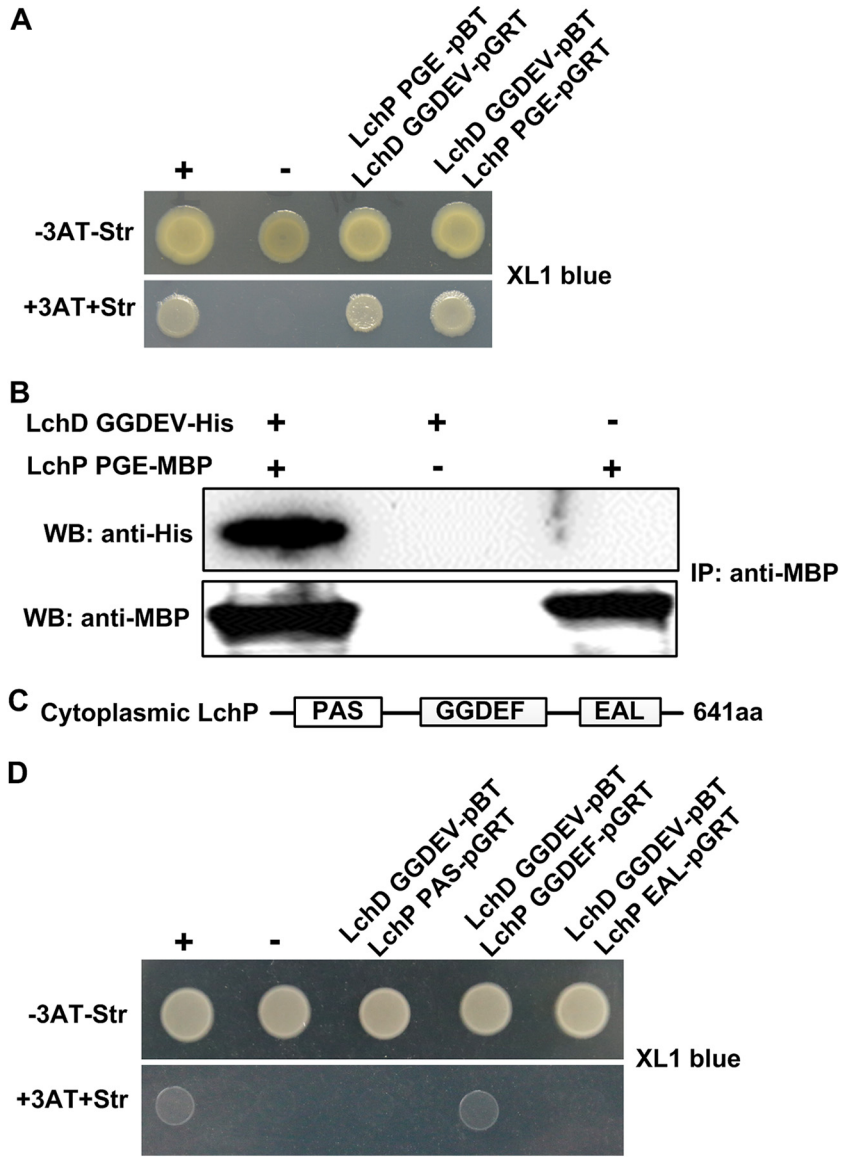

FIG 3 LchD physically interacts with LchP. (A) An *E. coli*-based B2H assay shows that the cytoplasmic regions of LchD and LchP interact. +, positive control (GacS-pBT and GacS-pTRG); −, negative control (vectors pBT and pTRG). (B) Diagram of LchP fragments. (C) Confirmation of the LchD and LchP interaction by a pulldown assay. The immunoprecipitation (IP) assay was carried out using anti-MBP antibody. Western blotting (WB) was performed by using anti-His and anti-MBP antibodies. (D) The B2H assay shows that the GGDEF domains of LchP and LchD interact. +, positive control (GacS-pBT and GacS-pTRG); −, negative control (vectors pBT and pTRG). aa, amino acids.

via pulldown of LchD-GGDEV-His using purified LchP-PGE-maltose binding protein (MBP) (27), which produced a positive signal (Fig. 3B). Both experiments strongly suggested that the cytoplasmic regions of LchP and LchD physically interact. To evaluate whether c-di-GMP is involved in the LchP-LchD interaction, we first detected it by the B2H system in the XL1-Blue *yhjH* mutant, which is considered to be a high-c-di-GMP-level background strain (15), and obtained results similar to those shown in Fig. 3A (Fig. S2A). More directly, we used a pulldown assay to compare the interactions between LchP and LchD in the presence and absence of c-di-GMP and found no difference (Fig. S2B). Considering that LchP has 3 cytoplasmic domains (Fig. 3C), to determine the details of this interaction, we further investigated which domain of LchP is involved in binding LchD-GGDEV with the B2H system. As shown in Fig. 3D, the two GGDEF domains interact. We also used the B2H system to determine whether the cytoplasmic regions of LchP and 1158 interacted;

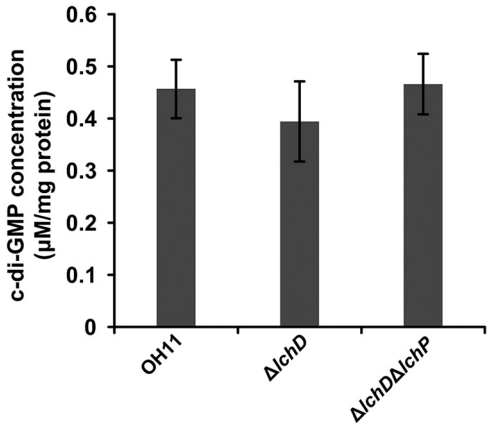

FIG 4 Quantification of intracellular c-di-GMP concentrations. The *lchD* mutant showed modestly decreased levels of intracellular c-di-GMP compared to those in the wild-type strain, while the *lchD* and *lchP* double mutant showed c-di-GMP levels restored to those detected in the wild-type strain. The data from three experiments are shown. Statistical comparisons were performed with GraphPad software (GraphPad, La Jolla, CA) using one-way ANOVA. The error bars indicate standard errors.

however, a negative result was obtained (Fig. S3). These results indicate that the LchP-LchD interaction is specific and may explain why only LchD participates in HSAF production in the absence of LchP, as shown in Fig. 2A.

LchD and LchP may regulate the local c-di-GMP concentration. Our previous study reported a very modest increase in the c-di-GMP concentration in the *lchP* mutant compared to the wild-type strain (27). A somewhat similar result was obtained in the present study. We collected *Lysobacter* strains in HSAF production medium (1/10 tryptic soy broth [TSB]) at the logarithmic growth phase (27), which is the same growth phase as that in the RNA-seq experiment, to detect the c-di-GMP levels. The results in Fig. 4 show that the concentration of c-di-GMP in the *lchD* mutant was slightly decreased compared to that in the wild-type strain (Fig. 4). Moreover, we measured the c-di-GMP level in the *lchD-lchP* double mutant and found that it was maintained as the level in the wild-type strain. Taken together, the results described above support that LchD may cooperate with LchP to control the local, but not global, c-di-GMP concentration to regulate HSAF biosynthesis.

The GGDEV active site is necessary for the regulation of HSAF biosynthesis. LchP contains both active GGDEF and EAL domains but utilizes its PDE activity to regulate HSAF biosynthesis (27). However, it is unclear whether the DGC activity of LchD is important for this process since the GGDEF domains of LchD and LchP interact (Fig. 3D).

The GGDEF motif is the known catalytic center of a DGC. We aimed to determine whether the regulation of HSAF biosynthesis would be retained upon the inactivation of the DGC activity of LchD. Therefore, we mutated the GGDEV active site of LchD to GGAAV to generate catalytically inactive LchD and used an *Escherichia coli*-based motility assay to detect the DGC activity of the mutant protein. The results in Fig. 5A show that the expression of the mutant LchD protein did not change the swimming area of *E. coli* MG1655, but the expression of the wild-type LchD protein decreased the swimming area due to an increase in the c-di-GMP level, indicating that mutant LchD was deficient in the DGC activity. Next, we overexpressed inactive *lchD* in the wild-type background and measured HSAF production. As shown in Fig. 5B, inactive LchD lost the ability to regulate HSAF biosynthesis since similar amounts of HSAF were produced by the strain overexpressing the inactivated mutant and the wild-type strain containing the pBBR vector. Furthermore, B2H assay data (Fig. 5C) indicated that the catalytically inactive LchD protein no longer interacted with LchP. Thus, regardless of the DGC activity of LchD or its interaction with LchP, the GGDEV active site plays a key role in the regulation of HSAF production.

Another structure that may contribute to LchD DGC activity is the conserved I-site RAYD (Fig. 2B). We constructed an RAYD inactive-site mutant, $LchD_{AAYA}$, and found that it created a smaller swimming area than the wild type, indicating that the mutant of the I-site relieved

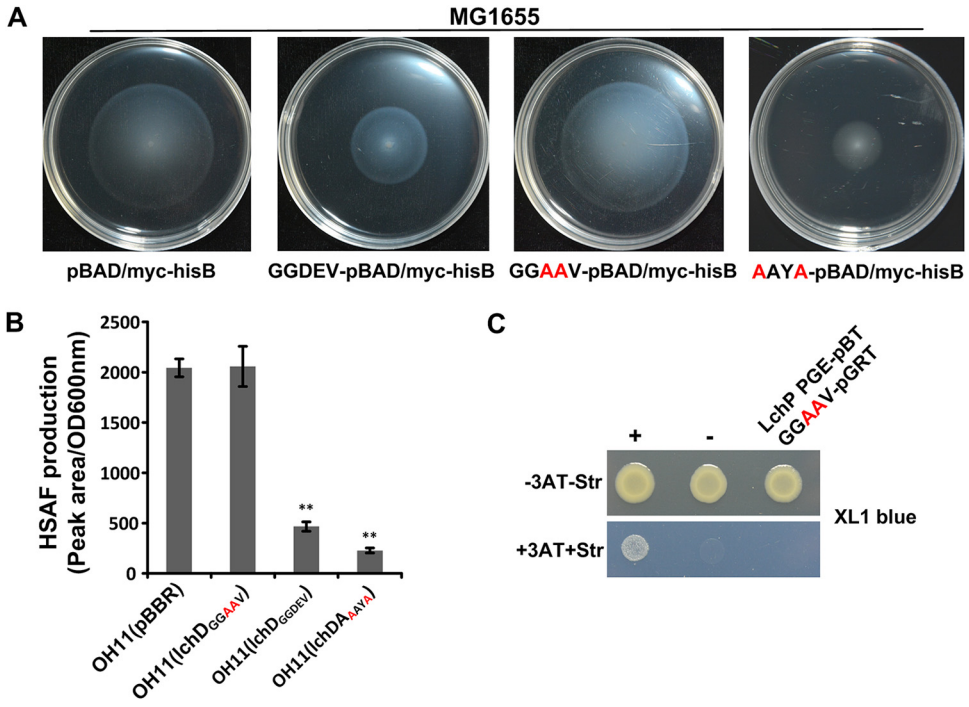

FIG 5 The catalytic center of LchD is important for complex formation with LchP and HSAF production. (A) An *E. coli*-based swimming motility assay indicated that mutant LchD does not have DGC activity and that the I-site mutant has stronger DGC activity. (B) Quantification of HSAF production by a series of mutant strains. Statistical comparisons were performed with GraphPad software (GraphPad, La Jolla, CA) using one-way ANOVA. (C) A B2H assay showed that mutant LchD does not interact with LchP. +, positive control (GacS-pBT and GacS-pTRG); −, negative control (vectors pBT and pTRG).

the inhibition of its DGC activity. Next, we overexpressed LchD$_{AAYA}$ in wild-type OH11, measured its HSAF production, and found that it was lower than the overexpression of wild-type LchD (Fig. 5B). We then purified LchD$_{AAYA}$ and used a protein pulldown assay to detect its interaction with LchP. The results in Fig. S2C show that the mutant of the I-site of LchD did not influence its interaction with LchP. We also evaluated the addition of c-di-GMP to the interaction system and found that c-di-GMP did not show any influence (Fig. S2B), which was consistent with the B2H results (Fig. 3A and Fig. S2A).

DISCUSSION

Our previous study investigated a specific c-di-GMP pathway involved in the biosynthesis of the antibiotic HSAF in the potential biocontrol agent *Lysobacter enzymogenes* OH11. In this pathway, the c-di-GMP PDE LchP and the c-di-GMP receptor Clp (which is also a transcription regulator) form a complex to ensure the specificity of c-di-GMP-mediated signaling (27). Clp is an important transcriptional regulator that participates in many processes in *L. enzymogenes* (28), indicating that Clp should be distributed throughout the whole cell. In the present study, RNA-seq data indicated that LchP specifically regulates HSAF biosynthesis. The inconsistent effects of Clp and LchP suggested that LchP may be a local c-di-GMP-hydrolyzing enzyme but not a global modulator. Thus, we aimed to identify the DGC that acts on the same local c-di-GMP signaling pathway.

Like excess water spilling out of a container, excess c-di-GMP can interfere with other functions. Therefore, we constructed DGC mutants based on the *lchP* mutant, but not overexpression strains, to directly target the specific c-di-GMP pathway associated with LchP and found only one DGC, LchD, out of 19 DGCs in *L. enzymogenes* OH11 that may modulate the same c-di-GMP pathway with LchP (Fig. 2A). B2H and protein pulldown assays showed that LchP physically interacts with LchD but does not interact with the similar DGC 1158 (see Fig. S3 in the supplemental material), indicating that LchP and LchD have the same subcellular

localization and confirming that LchP and LchD are partners that regulate the same c-di-GMP pathway.

An increasing number of recent studies have focused on local c-di-GMP signaling, and several mechanisms employed by some bacteria to maintain signaling specificity have been identified (22, 33). Because various types of N-terminal signal transduction domains are usually connected to a GGDEF or an EAL domain (5, 34), the activation of a given DGC or PDE by the desired signals at the desired time is a straightforward way to maintain c-di-GMP signaling specificity (35). The physical interaction among the c-di-GMP signaling components is another regulatory mechanism. An increasing number of examples have shown the interactions between DGCs, PDEs, and downstream receptors. Classic cases include but are not limited to the complexes formed by the PDE YciR and the DGC YdaM, the DGC DosC and the PDE DosP, and the DGC DgcC and the PDE PdeK from *E. coli* (19, 33, 36) and the DGC GcbC and the receptor LapD from *Pseudomonas fluorescens* (20). Physical interaction enables the delivery of c-di-GMP to a given target or the triggering of downstream targets in some cases. However, the mechanism by which signaling specificity is maintained by the formation of a complex between a DGC and a PDE remains unclear. Similar to LchP and LchD in the present study, deletion of only *lchD* (but not the 18 other DGCs) in the *lchP* mutant background restored HSAF production. Thus, this phenotype is consistent with the presence of a local c-di-GMP pool that is used to balance the concentration of c-di-GMP by LchP and LchD to trigger the downstream effector Clp, which activates HSAF biosynthesis to fight against filamentous fungi.

Although direct evidence showing the existence of a local c-di-GMP pool is lacking, there is a method that can measure the levels of another second messenger, cAMP, and cAMP gradients in real time with spatial accuracy in the nanometer range. Bock and colleagues used 8-FDA [2-(5(6)-carboxyfluoresceindiacetate)-aminoethylthio]-cAMP, the hydrolysis of which generates fluorescent 8-F-cAMP, which can be assayed by fluorescence fluctuation spectroscopy in combination with confocal microscopy (37). Using this method, the effects of binding sites on free cAMP concentrations in cells and on the spatial profile of cAMP gradients generated by PDE-mediated degradation could be analyzed. Those authors demonstrated that a low concentration of free cAMP enables PDEs to establish a local cAMP pool with a lower cAMP concentration below the activation threshold for the downstream effectors (37). Although cAMP signaling exists in eukaryotes, bacteria seem to employ an analogous strategy. We anticipate that a similar mechanism will be illustrated by bacteriologists in the near future.

MATERIALS AND METHODS

Strains, plasmids, and growth conditions. The bacterial strains and plasmids used in this study are listed in Table 1. *Lysobacter* strains were cultured in LB medium at 28°C unless stated otherwise. *E. coli* strains were cultured in LB medium at 37°C. Appropriate antibiotics (25 μg/mL kanamycin, 25 μg/mL gentamicin, 12.5 μg/mL tetracycline, 34 μg/mL chloramphenicol, and 8 μg/mL streptomycin [Str]) were used as needed.

Gene deletion and overexpression. In-frame gene deletion in *L. enzymogenes* OH11 was performed as described in our previous study (27). Briefly, the up- and downstream fragments of the target gene were amplified using the corresponding primers listed in Table 2 and cloned into the suicide vector pEX18GM (Table 1). The recombinant vector was transformed into the wild-type strain by electroporation. Via double-crossover homologous recombination, the in-frame target gene deletion mutant was then picked up by PCR and further confirmed by gene sequencing (TsingKe Biological Technology Company, Beijing, China).

Gene overexpression constructs were generated as described previously (38). The primers used in this study are listed in Table S1 in the supplemental material. In brief, the target gene and its predicted promoter were amplified by PCR and cloned into the broad-host-range vector pBBR1-MCS5 (Table 1). The construct was transformed into the wild-type strain by electroporation. The transformants were selected on LB agar plates containing gentamicin.

RNA-seq. Strains were cultured in LB medium at 28°C overnight, and 1 mL of the culture was transformed into 50 mL of 1/10 tryptic soy broth (TSB). Cells were collected at an optical density at 600 nm (OD_{600}) of 1.0. Next, clustering and sequencing were performed by BGI Genomics (Shenzhen, China). To analyze the differentially expressed genes between the *lchP* mutant and wild-type cells, the reads for all contigs were converted to reads per kilobase per million (RPKM) (39). The expression abundance of each contig in the two samples was calculated using the MARS (MA plot-based method with random sampling ["MA" indicating M values versus log-intensity averages {A values}]) model by the differentially expressed gene seq package. Differentially expressed genes between the *lchP* mutant strain and the wild-type strain were identified by DEGseq software (40). The FDR (false discovery rate) was used to determine the *P* value threshold for the analysis. An FDR of $\leq$0.001 and a $\log_2$ fold change of greater than 1.0 or less than -1.0 were used to indicate a significant change in the expression abundance.

TABLE 1 Strains and plasmids used in this study

Strain or plasmid	Characteristic(s)[a]	Reference or source
Strains		
Lysobacter enzymogenes		
OH11	Wild type; Km^r	46
Δ*3756* (Δ*lchD*)	*le3756* in-frame deletion mutant	This study
Δ*2762* (Δ*lchP*)	*lchP* in-frame deletion mutant	27
Δ*0082* Δ*lchP*	*le0082* and *lchP* double-deletion mutant	This study
Δ*4875* Δ*lchP*	*le4875*and *lchP* double-deletion mutant	This study
Δ*3882* Δ*lchP*	*le3882* and *lchP* double-deletion mutant	This study
Δ*0901* Δ*lchP*	*le0901* and *lchP* double-deletion mutant	This study
Δ*2826* Δ*lchP*	*le2826* and *lchP* double-deletion mutant	This study
Δ*0155* Δ*lchP*	*le0155* and *lchP* double-deletion mutant	This study
Δ*2120* Δ*lchP*	*le2120* and *lchP* double-deletion mutant	This study
Δ*3756* Δ*lchP*	*le3756* and *lchP* double-deletion mutant	This study
Δ*1158* Δ*lchP*	*le1158* and *lchP* double-deletion mutant	This study
OH11(pBBR)	Vector control	This study
OH11(LchD)	Vector-based *lchD* overexpression strain	This study
OH11(LchD$_{GGAAV}$)	Site-mutated *lchD* overexpression strain	This study
Escherichia coli		
TOP10	*supE44 lacU169*(Δ*lacZ*ΔM15) *hsdR17 recA1 endA1 gyrA96 thi-1 relA11*	47
MG1655	Wild type	ATCC 700926a
XL1-Blue MRF′	Δ(*mcrA 183 83mcrCB-hsdSMR-mrr*) *173 endA1 supE44 thi-1 recA1 gyrA96 relA1 lac* {F[*3proAB lacI*^{q}ZΔM15 Tn*10* (Tet^r)]}	43
BL21(DE3)	Host strain for protein expression; Km^r	TaKaRa Company, Shanghai, China
Plasmids		
pEX18GM	Suicide vector for gene in-frame deletion; Gm^r	48
0082-pEX18	Plasmid for in-frame deletion of *le0082*	This study
4875-pEX18	Plasmid for in-frame deletion of *le4875*	27
3882-pEX18	Plasmid for in-frame deletion of *le3882*	27
0901-pEX18	Plasmid for in-frame deletion of *le0901*	This study
2826-pEX18	Plasmid for in-frame deletion of *le2826*	This study
0155-pEX18	Plasmid for in-frame deletion of *le0155*	27
2120-pEX18	Plasmid for in-frame deletion of *le2120*	This study
3756-pEX18	Plasmid for in-frame deletion of *le3756*	This study
1158-pEX18	Plasmid for in-frame deletion of *le1158*	This study
pBBR1-MCS5	Broad-host-range vector for gene overexpression; Gm^r	49
lchD-pBBR	Plasmid for LchD overexpression	This study
lchD$_{GGAAV}$-pBBR	Plasmid for site-mutated LchD overexpression	This study
pBAD/Myc-His B	Vector for arabinose-inducible expression; Amp^r	Invitrogen
GGDEV-pBAD	pBAD/Myc-His B containing the cytoplasmic part of LchD	This study
GGAAV-pBAD	pBAD/Myc-His B containing mutated LchD	This study
pTRG	Plasmid for protein expression in the bacterial two-hybrid assay; Tet^r	50
LchP-pTRG	pTRG containing the cytoplasmic part of LchP	27
LchD-pTRG	pTRG containing the cytoplasmic part of LchD	This study
PAS-pTRG	pTRG containing the PAS domain of LchP	This study
GGDEF-pTRG	pTRG containing the GGDEF domain of LchP	This study
EAL-pTRG	pTRG containing the EAL domain of LchP	This study
GGAAV-pTRG	pTRG containing site-mutated LchD	This study
1158-pTRG	pTRG containing Le1158	This study
pBT	Plasmid for protein expression in bacterial two-hybridization assays; Chlo^r	50
LchP-pBT	pBT containing the cytoplasmic part of LchP	27
LchD-pBT	pBT containing the cytoplasmic part of LchD	This study
pMAL-p2x	Vector for expression of the MBP tag fusion protein	Huayue Company, Beijing, China
LchP-pMAL-p2x	pMAL-p2x::LchP PAS+GGDEF+EAL	27
pET30a(+)	Vector for expression of the His tag fusion protein	TaKaRa Company
LchD-pET30a	pET30a::*lchD GGDEV*	This study

[a]Km^r, Gm^r, Amp^r, Tet^r, and Chlo^r represent kanamycin, gentamicin, ampicillin, tetracycline, and chloramphenicol resistance, respectively.

qRT-PCR. Strains were cultured in LB medium at 28°C overnight. One milliliter of the culture was transferred to 50 mL of 1/10 TSB, and cells were collected at an OD_{600} of 1.0. RNA extraction was performed with a bacterial RNA kit (Omega, China), and RNA concentrations were measured with a Nanodrop ND-1000 UV spectrophotometer (Thermo Fisher, USA). cDNA was generated using a PrimeScript RT reagent kit with gDNA Eraser (TaKaRa, Japan) according to the manufacturer's protocol. qRT-PCR was performed using an Applied

TABLE 2 Primers used in this study

Primer	Sequence (restriction enzyme)[a]	Purpose
Primers used for gene in-frame deletion		
0155F1	CCCAAGCTTCGCAGCAGATGGGCAGCTAT (HindIII)	To amplify a 710-bp upstream homologue arm of *le0155*
0155R1	GGGGTACCGCGGCGACTTCATTCCACCT (KpnI)	
0155F2	GGGGTACCCGCAGTTGCCTTGAGTCGAG (KpnI)	To amplify a 636-bp downstream homologue arm of *le0155*
0155R2	GCTCTAGAGCTGTTGTTCGTCTCCACCC (XbaI)	
0082F1	CCCAAGCTTGCGGCTACTTCTGGCGGGTG (HindIII)	To amplify a 538-bp upstream homologue arm of *le0082*
0082R1	CGGAATTCTAGCCCCAGTGCGAGAGGTG (EcoRI)	
0082F2	CGGAATTCCGGTTGGGGGAGGTTTGAGC (EcoRI)	To amplify a 485-bp downstream homologue arm of *le0082*
0082R2	GCTCTAGAGGCTGGGGGGTGTTGAGAGG (XbaI)	
4875F1	CCCAAGCTTTCACCACCAAGGACTACCGC (HindIII)	To amplify a 692-bp upstream homologue arm of *le4875*
4875R1	GGGGTACCCGCCACCAGATTGCCGTTGT (KpnI)	
4875F2	GGGGTACCGAGGATTTCGCCGTGCAGGT (KpnI)	To amplify a 421-bp downstream homologue arm of *le4875*
4875R2	GCTCTAGAGATCGTGGTCTTGTCGGCGC (XbaI)	
3882F1	CCCAAGCTTACGAACAGGGCTACGAACGC (HindIII)	To amplify a 686-bp upstream homologue arm of *le3882*
3882R1	GGGGTACCCGGAGGCTGTGTCGTTCGCG (KpnI)	
3882F2	GGGGTACCGTCCGCCACTGACCGCTCGC (KpnI)	To amplify a 300-bp downstream homologue arm of *le3882*
3882R2	GCTCTAGACGTTGCTGGGCGAGTGCTTC (XbaI)	
0901F1	CCCAAGCTTCCTTCATCCTGCCGACCAGT (HindIII)	To amplify a 784-bp upstream homologue arm of *le0901*
0901R1	GGGGTACCATGTCGTCGTAGGCGCTCTC (KpnI)	
0901F2	GGGGTACCCGCCTGGTTGCCGACGAGGG (KpnI)	To amplify a 616-bp downstream homologue arm of *le0901*
0901R2	GCTCTAGACGGCAGCGGGAAACTCAGGC (XbaI)	
2826F1	CCCAAGCTTAAGGCGGTCGGCGTGGTGAT (HindIII)	To amplify a 625-bp upstream homologue arm of *le2826*
2826R1	GGGGTACCCACCGCCATCACCAGCAAGC (KpnI)	
2826F2	GGGGTACCGCTTCTGATACGGCTCCTGC (KpnI)	To amplify a 616-bp downstream homologue arm of *le2826*
2826R2	GCTCTAGAGATGGCGGCGAACTGGCGAT (XbaI)	
2120F1	CCCAAGCTTCGAGCGAAGGCGGATGGATG (HindIII)	To amplify a 522-bp upstream homologue arm of *le2120*
2120R1	GGGGTACCACCGCCATCGCCACATCCGT (KpnI)	
2120F2	GGGGTACCAGTTCTGCCTGCTGGTCGCC (KpnI)	To amplify an 854-bp upstream homologue arm of *le2120*
2120R2	GCTCTAGAATCTCCTGCGGCTCGGGCAC (XbaI)	
3756F1	CCCAAGCTTCGCCGCCCCCTGTCGTTTTT (HindIII)	To amplify a 273-bp upstream homologue arm of *le3756*
3756R1	GGGGTACCTCGTCGCCACCGCCCACAAC (KpnI)	
3756F2	GGGGTACCAGCGAGAGCGAACACGAGGT (KpnI)	To amplify a 510-bp upstream homologue arm of *le3756*
3756R2	GCTCTAGACCAGGCAGCGGTAGACGAAT (XbaI)	
1158F1	CCCAAGCTTATCGCCACTTCCTCCACCGC (HindIII)	To amplify a 535-bp upstream homologue arm of *le1158*
1158R1	GCTCTAGAAGGACCACGACACCGCCAAG (XbaI)	
1158F2	GCTCTAGAGCCAGGACCGTTCCATTTCC (XbaI)	To amplify a 564-bp upstream homologue arm of *le1158*
1158R2	GGGGTACCAGGGGGCGGGCTGAGAGGAC (KpnI)	
Primers used for gene overexpression		
cp3756F	CCCAAGCTTCGCCGCCCCCTGTCGTTTTT (HindIII)	To amplify a 2,235-bp fragment of *le3756* and its predicted promoter
cp3756R	GCTCTAGAGTTTCGATCAGGTAGCCCGC (XbaI)	

(Continued on next page)

TABLE 2 (Continued)

Primer	Sequence (restriction enzyme)[a]	Purpose
Primers used for DGC activity assay		
GGDEV-F	GGGGTACCAAGCTGCAACAGCTGCG (KpnI)	To amplify a 561-bp fragment encoding the LchD cytoplasmic domain
GGDEV-R	CCCAAGCTTTCAAGAGACCACCTCGTGTT (HindIII)	
Primers used for bacterial two-hybrid assay		
GGDEV-F(T)	CGGGATCCAAGCTGCAACAGCTGCGTCG (BamHI)	To amplify a 561-bp fragment encoding the LchD cytoplasmic domain
GGDEV-R(T)	CCGCTCGAGCCGGTCGCGGCCGGCGGACT (XhoI)	
PAS-F	CGGGATCCGACGATCACGAGATCCATCC (BamHI)	To amplify a 579-bp fragment encoding the PAS domain of LchP
PAS-R	CCGCTCGAGGTCGGTGATGTCGGTCAGCA (XhoI)	
GGDEF-F	CGGGATCCGCCAACTACGACACCCTCAC (BamHI)	To amplify a 477-bp fragment encoding the GGDEF domain of LchP
GGDEF-R	CCGCTCGAGGGTGCGCCGGCCGGCGGCCT (XhoI)	
EAL-F	CGGGATCCTCCGCGGCGCTGCGCAAGGT (BamHI)	To amplify a 711-bp fragment encoding the EAL domain of LchP
EAL-R	CCGCTCGAGCGGCTTGGCCAGCCAGTAGC (XhoI)	
1158-F(PTRG)	CGGGATCCGCCAAGCTGCAGAAGCTGCG (BamHI)	To amplify a 561-bp fragment encoding the 1158 cytoplasmic domain
1158-R(PTRG)	CCGCTCGAGTCAGATCGCCACTTCCTCCA (XhoI)	
Primers used for qRT-PCR		
pksF	ACTATTTGTTGGGCGACGAC	To detect the transcript level of *pks*
pksR	GTAACCGAACAGGGTGCAAT	
16sRNAF	ACGGTCGCAAGACTGAAACT	Reference gene
16sRNAR	AAGGCACCAATCCATCTCTG	
Primers used for protein expression		
LchD-His-F	GGAATTCCATATGAAGCTGCAACAGCTGCG (NdeI)	To amplify a 561-bp fragment encoding the LchD cytoplasmic domain
LchD-His-R	CCCAAGCTTTCAAGAGACCACCTCGTGTT (HindIII)	

[a]Restricted digestion enzyme sites are underlined.

Biosystems 7500 system, and the 16S rRNA gene was used as an internal control, as described previously (41). The primers used in this study are listed in Table 2.

HSAF extraction and detection. HSAF extraction and quantification were performed as described previously (42). In brief, HSAF was extracted from *L. enzymogenes* cultures in 1/10 TSB with an equal volume of ethyl acetate. HSAF was detected by HPLC (high-performance liquid chromatography) and quantified per OD_{600} unit. Biological experiments for each treatment were performed three times and assayed in triplicate.

DGC activity assay. The DGC activity assay was based on an *E. coli* motility reporter system as described previously (27). Briefly, the gene encoding the DGC under analysis was cloned into the pBAD/Myc-His B vector (Table 1). The construct was transformed into the *E. coli* MG1655 strain. Next, the swimming zone of the MG1655 strain expressing the construct or the original vector was observed on LB soft agar plates (0.25% agar) supplemented with 0.1% arabinose. Three biological replicates were tested.

Bacterial two-hybrid assay. The bacterial two-hybrid (B2H) assay was performed according to the protocol of the BacterioMatch II two-hybrid system (Agilent Technologies, USA). Genes encoding the target proteins were cloned into the pBT and pTGR plasmids and transformed into *E. coli* XL1-Blue MRF′ Kan. *E. coli* XL1-Blue MRF′ Kan containing the original pBT and pTGR plasmids served as a negative control, and the strain containing pBT-GacS and pTRG-GacS served as a positive control (43). All cotransformants were spotted onto selective plates and grown at 28°C for 48 h. According to the protocol from the kit manufacturer, selective plates contained 3-amino-1,2,4-triazole (3-AT) and Str to enable the growth of the positive colonies and disable the growth of the negative colonies. Three biological replicates were performed.

Protein expression and purification. The gene encoding cytoplasmic LchD was amplified and cloned into pET-30a(+) (Table 1). The construct was transformed into *E. coli* strain BL21(DE3) (Table S1) for protein expression and purification. Two milliliters of the culture grown overnight was transferred to 200 mL of fresh LB medium at 37°C and grown with shaking at 200 rpm to an OD_{600} of 0.6. Subsequently, isopropyl β-D-1-thiogalactopyranoside (IPTG; Sigma) was added to the culture to a final concentration of 0.5 mM, followed by growth at 28°C for 4 h. The cells were collected by centrifugation (13,000 rpm) at 4°C and sonicated using a 250 sonifier (Branson digital sonifier). After centrifugation, the soluble proteins were mixed with preequilibrated Ni^{2+} resin (GE Healthcare, Shanghai, China), and the target protein was eluted with 250 mM imidazole. Protein purity was assessed by SDS-PAGE, and the protein concentration was determined using a bicinchoninic acid (BCA) assay kit (TransGen Biotech, China).

Pulldown assay. Purified His-fused LchD-GGDEV and MBP-fused LchP-PGE (27) were subjected to a pulldown assay. The reaction system contained 800 μL of phosphate-buffered saline (PBS) with 5 μM LchD-GGDEV-His and LchP-PGE-MBP and 50 μL of amylose resin. Samples were incubated at 4°C overnight. The resins were collected by centrifugation and washed 10 times with PBS containing 1% Triton X-100 to remove unbound proteins. The immunoprecipitated proteins were eluted by boiling in the presence of 6× SDS loading dye for 10 min. Western blotting was performed using specific anti-MBP (catalogue number ab49923) and anti-His (catalogue number ab18184) antibodies from Abcam.

c-di-GMP extraction and quantification. c-di-GMP extraction and quantification were performed as described previously (27). Cultures were grown in 1/10 TSB at 28°C to an OD_{600} of 1.5. c-di-GMP was extracted with 0.6 M $HClO_4$ and 2.5 M K_2CO_3 as described previously (44, 45). Two milliliters of the cells was harvested for protein quantification by the BCA assay (TransGen Biotech, China). The samples were analyzed by liquid chromatography-mass spectrometry (LC-MS) on an Agilent 6460 triple-quadrupole LC-MS instrument.

Statistical analysis. Some experiments included in this study were performed three times with three replicates each. The means from three replicates are shown, with error bars indicating standard errors. Statistical comparisons were performed with GraphPad software (GraphPad, La Jolla, CA) using one-way analysis of variance (ANOVA). A P value of <0.05 was used to indicate significance.

Data availability. RNA-seq data have been uploaded to the Sequence Read Archive in the NCBI database with accession number PRJNA716139.

SUPPLEMENTAL MATERIAL

Supplemental material is available online only.

SUPPLEMENTAL FILE 1, PDF file, 0.6 MB.

ACKNOWLEDGMENTS

We thank Jialei Wang and Ning Wang from the Central Laboratory at the Jiangsu Academy of Agricultural Sciences for their technical support with the LC-MS (HPLC) analysis.

This study was funded by the National Natural Science Foundation of China (numbers 31901931 and 31872018), the Natural Science Foundation of Jiangsu Province (number BK20190266), and the China Agriculture Research System of MOF and MARA.

G.X. contributed to conceptualization, investigation, writing and editing the manuscript, and funding acquisition. G.X. carried out the experiments and analyzed data. L.Z. contributed to RNA-seq data analysis. G.Q. modified the main body of the manuscript. F.L. contributed to reviewing the manuscript, supervision, and funding acquisition. All authors contributed to the article and approved the submitted version.

REFERENCES

1. Ross P, Weinhouse H, Aloni Y, Michaeli D, Weinberger-Ohana P, Mayer R, Braun S, de Vroom E, van der Marel GA, van Boom JH, Benziman M. 1987. Regulation of cellulose synthesis in *Acetobacter xylinum* by cyclic diguanylic acid. Nature 325:279–281. https://doi.org/10.1038/325279a0.
2. Jenal U, Malone J. 2006. Mechanisms of cyclic-di-GMP signaling in bacteria. Annu Rev Genet 40:385–407. https://doi.org/10.1146/annurev.genet.40.110405.090423.
3. Romling U, Amikam D. 2006. Cyclic di-GMP as a second messenger. Curr Opin Microbiol 9:218–228. https://doi.org/10.1016/j.mib.2006.02.010.
4. Hengge R. 2009. Principles of cyclic-di-GMP signaling in bacteria. Nat Rev Microbiol 7:263–273. https://doi.org/10.1038/nrmicro2109.
5. Romling U, Galperin MY, Gomelsky M. 2013. Cyclic di-GMP: the first 25 years of a universal bacterial second messenger. Microbiol Mol Biol Rev 77:1–52. https://doi.org/10.1128/MMBR.00043-12.
6. Chan C, Paul R, Samoray D, Amiot N, Giese B, Jenal U, Schirmer T. 2004. Structural basis of activity and allosteric control of diguanylate cyclase. Proc Natl Acad Sci U S A 101:17084–17089. https://doi.org/10.1073/pnas.0406134101.
7. Paul R, Weiser S, Amiot NC, Chan C, Schirmer T, Giese B, Jenal U. 2004. Cell cycle-dependent dynamic localization of a bacterial response regulator with a novel di-guanylate cyclase output domain. Genes Dev 18:715–727. https://doi.org/10.1101/gad.289504.
8. Christen M, Christen B, Folcher M, Schauerte A, Jenal U. 2005. Identification and characterization of a cyclic di-GMP-specific phosphodiesterase and its allosteric control by GTP. J Biol Chem 280:30829–30837. https://doi.org/10.1074/jbc.M504429200.
9. Schmidt AJ, Ryjenkov DA, Gomelsky M. 2005. The ubiquitous protein domain EAL is a cyclic diguanylate-specific phosphodiesterase: enzymatically active and inactive EAL domains. J Bacteriol 187:4774–4781. https://doi.org/10.1128/JB.187.14.4774-4781.2005.
10. Tamayo R, Tischler AD, Camilli A. 2005. The EAL domain protein VieA is a cyclic diguanylate phosphodiesterase. J Biol Chem 280:33324–33330. https://doi.org/10.1074/jbc.M506500200.
11. Bellini D, Caly DL, McCarthy Y, Bumann M, An SQ, Dow JM, Ryan RP, Walsh MA. 2014. Crystal structure of an HD-GYP domain cyclic-di-GMP phosphodiesterase reveals an enzyme with a novel trinuclear catalytic iron centre. Mol Microbiol 91:26–38. https://doi.org/10.1111/mmi.12447.
12. Liang ZX. 2015. The expanding roles of c-di-GMP in the biosynthesis of exopolysaccharides and secondary metabolites. Nat Prod Rep 32:663–683. https://doi.org/10.1039/c4np00086b.
13. Ryjenkov DA, Simm R, Romling U, Gomelsky M. 2006. The PilZ domain is a receptor for the second messenger c-di-GMP: the PilZ domain protein YcgR controls motility in enterobacteria. J Biol Chem 281:30310–30314. https://doi.org/10.1074/jbc.C600179200.
14. Duerig A, Abel S, Folcher M, Nicollier M, Schwede T, Amiot N, Giese B, Jenal U. 2009. Second messenger-mediated spatiotemporal control of protein degradation regulates bacterial cell cycle progression. Genes Dev 23:93–104. https://doi.org/10.1101/gad.502409.
15. Fang X, Ahmad I, Blanka A, Schottkowski M, Cimdins A, Galperin MY, Römling U, Gomelsky M. 2014. GIL, a new c-di-GMP-binding protein domain involved in regulation of cellulose synthesis in enterobacteria. Mol Microbiol 93:439–452. https://doi.org/10.1111/mmi.12672.
16. Wang YC, Chin KH, Tu ZL, He J, Jones CJ, Sanchez DZ, Yildiz FH, Galperin MY, Chou SH. 2016. Nucleotide binding by the widespread high-affinity cyclic di-GMP receptor MshEN domain. Nat Commun 7:12481. https://doi.org/10.1038/ncomms12481.
17. Ha D-G, Richman ME, O'Toole GA. 2014. Deletion mutant library for investigation of functional outputs of cyclic diguanylate metabolism in *Pseudomonas aeruginosa* PA14. Appl Environ Microbiol 80:3384–3393. https://doi.org/10.1128/AEM.00299-14.

18. Newell PD, Yoshioka S, Hvorecny KL, Monds RD, O'Toole GA. 2011. Systematic analysis of diguanylate cyclases that promote biofilm formation by *Pseudomonas fluorescens* Pf0-1. J Bacteriol 193:4685–4698. https://doi.org/10.1128/JB.05483-11.
19. Lindenberg S, Klauck G, Pesavento C, Klauck E, Hengge R. 2013. The EAL domain protein YciR acts as a trigger enzyme in a c-di-GMP signaling cascade in *E. coli* biofilm control. EMBO J 32:2001–2014. https://doi.org/10.1038/emboj.2013.120.
20. Dahlstrom KM, Giglio KM, Collins AJ, Sondermann H, O'Toole GA. 2015. Contribution of physical interactions to signaling specificity between a diguanylate cyclase and its effector. mBio 6:e01978-15. https://doi.org/10.1128/mBio.01978-15.
21. Valentini M, Laventie BJ, Moscoso J, Jenal U, Filloux A. 2016. The diguanylate cyclase HsbD intersects with the HptB regulatory cascade to control *Pseudomonas aeruginosa* biofilm and motility. PLoS Genet 12:e1006354. https://doi.org/10.1371/journal.pgen.1006354.
22. Römling U, Gomelsky M, Galperin MY. 2005. C-di-GMP: the dawning of a novel bacterial signalling system. Mol Microbiol 57:629–639. https://doi.org/10.1111/j.1365-2958.2005.04697.x.
23. Li S, Du L, Yuen G, Harris SD. 2006. Distinct ceramide synthases regulate polarized growth in the filamentous fungus *Aspergillus nidulans*. Mol Biol Cell 17:1218–1227. https://doi.org/10.1091/mbc.e05-06-0533.
24. Yu F, Zaleta-Rivera K, Zhu X, Huffman J, Millet JC, Harris SD, Yuen G, Li XC, Du L. 2007. Structure and biosynthesis of heat-stable antifungal factor (HSAF), a broad-spectrum antimycotic with a novel mode of action. Antimicrob Agents Chemother 51:64–72. https://doi.org/10.1128/AAC.00931-06.
25. Lou L, Qian G, Xie Y, Hang J, Chen H, Zaleta-Rivera K, Li Y, Shen Y, Dussault PH, Liu F, Du L. 2011. Biosynthesis of HSAF, a tetramic acid-containing macrolactam from *Lysobacter enzymogenes*. J Am Chem Soc 133:643–645. https://doi.org/10.1021/ja105732c.
26. Chen Y, Xia J, Su Z, Xu G, Gomelsky M, Qian G, Liu F. 2017. *Lysobacter* PilR, the regulator of type IV pilus synthesis, controls antifungal antibiotic production via a cyclic di-GMP pathway. Appl Environ Microbiol 83:e03397-16. https://doi.org/10.1128/AEM.03397-16.
27. Xu G, Han S, Huo C, Chin KH, Chou SH, Gomelsky M, Qian G, Liu F. 2018. Signaling specificity in the c-di-GMP-dependent network regulating antibiotic synthesis in *Lysobacter*. Nucleic Acids Res 46:9276–9288. https://doi.org/10.1093/nar/gky803.
28. Wang Y, Zhao Y, Zhang J, Zhao Y, Shen Y, Su Z, Xu G, Du L, Huffman JM, Venturi V, Qian G, Liu F. 2014. Transcriptomic analysis reveals new regulatory roles of Clp signaling in secondary metabolite biosynthesis and surface motility in *Lysobacter enzymogenes* OH11. Appl Microbiol Biotechnol 98:9009–9020. https://doi.org/10.1007/s00253-014-6072-1.
29. Galperin MY, Nikolskaya AN, Koonin EV. 2001. Novel domains of the prokaryotic two-component signal transduction systems. FEMS Microbiol Lett 203:11–21. https://doi.org/10.1111/j.1574-6968.2001.tb10814.x.
30. Ren X, Ren S, Xu G, Dou W, Chou SH, Chen Y, Qian G. 2020. Knockout of diguanylate cyclase genes in *Lysobacter enzymogenes* to improve production of antifungal factor and increase its application in seed coating. Curr Microbiol 77:1006–1015. https://doi.org/10.1007/s00284-020-01902-x.
31. Anantharaman V, Aravind L. 2003. Application of comparative genomics in the identification and analysis of novel families of membrane-associated receptors in bacteria. BMC Genomics 4:34. https://doi.org/10.1186/1471-2164-4-34.
32. Joung JK, Ramm EI, Pabo CO. 2000. A bacterial two-hybrid selection system for studying protein-DNA and protein-protein interactions. Proc Natl Acad Sci U S A 97:7382–7387. https://doi.org/10.1073/pnas.110149297.
33. Richter AM, Possling A, Malysheva N, Yousef KP, Herbst S, von Kleist M, Hengge R. 2020. Local c-di-GMP signaling in the control of synthesis of the *E. coli* biofilm exopolysaccharide pEtN-cellulose. J Mol Biol 432:4576–4595. https://doi.org/10.1016/j.jmb.2020.06.006.
34. Cruz DP, Huertas MG, Lozano M, Zárate L, Zambrano MM. 2012. Comparative analysis of diguanylate cyclase and phosphodiesterase genes in *Klebsiella pneumoniae*. BMC Microbiol 12:139. https://doi.org/10.1186/1471-2180-12-139.
35. Dahlstrom KM, O'Toole GA. 2017. A symphony of cyclases: specificity in diguanylate cyclase signaling. Annu Rev Microbiol 71:179–195. https://doi.org/10.1146/annurev-micro-090816-093325.
36. Tuckerman JR, Gonzalez G, Sousa EH, Wan X, Saito JA, Alam M, Gilles-Gonzalez MA. 2009. An oxygen-sensing diguanylate cyclase and phosphodiesterase couple for c-di-GMP control. Biochemistry 48:9764–9774. https://doi.org/10.1021/bi901409g.
37. Bock A, Annibale P, Konrad C, Hannawacker A, Anton SE, Maiellaro I, Zabel U, Sivaramakrishnan S, Falcke M, Lohse MJ. 2020. Optical mapping of cAMP signaling at the nanometer scale. Cell 182:1519–1530. https://doi.org/10.1016/j.cell.2020.07.035.
38. Xu G, Shi X, Wang R, Xu H, Du L, Chou SH, Liu H, Liu Y, Qian G, Liu F. 2018. Insights into the distinct cooperation between the transcription factor Clp and *Le*DSF signaling in the regulation of antifungal factors in *Lysobacter enzymogenes* OH11. Biol Control 120:52–58. https://doi.org/10.1016/j.biocontrol.2016.08.006.
39. Mortazavi A, Williams BA, McCue K, Schaeffer L, Wold B. 2008. Mapping and quantifying mammalian transcriptomes by RNA-Seq. Nat Methods 5:621–628. https://doi.org/10.1038/nmeth.1226.
40. Wang L, Feng Z, Wang X, Wang X, Zhang X. 2010. DEGseq: an R package for identifying differentially expressed genes from RNA-seq data. Bioinformatics 26:136–138. https://doi.org/10.1093/bioinformatics/btp612.
41. Qian G, Wang Y, Liu Y, Xu F, He Y, Du L, Venturi V, Fan J, Hu B, Liu F. 2013. *Lysobacter enzymogenes* uses two distinct cell-cell signaling systems for differential regulation of secondary-metabolite biosynthesis and colony morphology. Appl Environ Microbiol 79:6604–6616. https://doi.org/10.1128/AEM.01841-13.
42. Qian G, Xu F, Venturi V, Du L, Liu F. 2014. Roles of a solo LuxR in the biological control agent *Lysobacter enzymogenes* strain OH11. Phytopathology 104:224–231. https://doi.org/10.1094/PHYTO-07-13-0188-R.
43. Guo M, Feng H, Zhang J, Wang W, Wang Y, Li Y, Gao C, Chen H, Feng Y, He Z. 2009. Dissecting transcription regulatory pathways through a new bacterial one-hybrid reporter system. Genome Res 19:1301–1308. https://doi.org/10.1101/gr.086595.108.
44. Hickman JW, Harwood CS. 2008. Identification of FleQ from *Pseudomonas aeruginosa* as a c-di-GMP-responsive transcription factor. Mol Microbiol 69:376–389. https://doi.org/10.1111/j.1365-2958.2008.06281.x.
45. Zhu B, Liu C, Liu S, Cong H, Chen Y, Gu L, Ma LZ. 2016. Membrane association of SadC enhances its diguanylate cyclase activity to control exopolysaccharides synthesis and biofilm formation in *Pseudomonas aeruginosa*. Environ Microbiol 18:3440–3452. https://doi.org/10.1111/1462-2920.13263.
46. Qian G, Hu B, Jiang Y, Liu F. 2009. Identification and characterization of *Lysobacter enzymogenes* as a biological control agent against some fungal pathogens. Agr Sci China 8:68–75. https://doi.org/10.1016/S1671-2927(09)60010-9.
47. Han Y, Wang Y, Tombosa S, Wright S, Huffman J, Yuen G, Qian G, Liu F, Shen Y, Du L. 2015. Identification of a small molecule signaling factor that regulates the biosynthesis of the antifungal polycyclic tetramate macrolactam HSAF in *Lysobacter enzymogenes*. Appl Microbiol Biotechnol 99:801–811. https://doi.org/10.1007/s00253-014-6120-x.
48. Hoang TT, Karkhoff-Schweizer RR, Kutchma AJ, Schweizer HP. 1998. A broad-host-range Flp-FRT recombination system for site-specific excision of chromosomally-located DNA sequences: application for isolation of unmarked Pseudomonas aeruginosa mutants. Gene 212:77–86. https://doi.org/10.1016/s0378-1119(98)00130-9.
49. Kovach ME, Elzer PH, Hill DS, Robertson GT, Farris MA, Roop RM, II, Peterson KM. 1995. Four new derivatives of the broad-host-range cloning vector pBBR1MCS, carrying different antibiotic-resistance cassettes. Gene 166:175–176. https://doi.org/10.1016/0378-1119(95)00584-1.
50. Fang X, Gomelsky M. 2010. A post-translational, c-di-GMP-dependent mechanism regulating flagella motility. Mol Microbiol 76:1295–1305. https://doi.org/10.1111/j.1365-2958.2010.07179.x.